THIRD UK CONFERENCE ON BOUNDARY INTEGRAL METHODS

Editor:
P. J. Harris
School of Computing and Mathematical Sciences
University of Brighton
Lewes Road
Brighton BN2 4GJ
U.K.

Held at:
University of Brighton
10-11 September 2001.

Published by University of Brighton Press
ISBN 1-901177-32-7

A BOUNDARY ELEMENT INVESTIGATION OF THE POTENTIAL BOUNDARY DETERMINATION

D. Lesnic*†, J.R. Berger** and P.A. Martin*
*Department of Mathematical and Computer Sciences** and Division of Engineering***,
Colorado School of Mines, Golden, CO 80401-1887, USA
† On study leave from *Department of Applied Mathematics, University of Leeds, Leeds LS2 9JT, UK*

Abstract
The inverse problem for the Laplace equation which requires the determination of the location, size and shape of an unknown portion $\gamma \subset \partial\Omega$ of the boundary $\partial\Omega$ of a solution domain $\Omega \subset R^2$ from Cauchy data on the remaining portion of the boundary $\Gamma = \partial\Omega - \gamma$ is considered. This situation arises in the study of quantitative non-destructive evaluation of corrosion in materials in which boundary measurements of currents and voltages are used to determine the material loss caused by corrosion. The Laplace equation is discretised using the boundary element method (BEM) and constrained minimization problems based on least-squares, zeroth- or first-order regularization are formulated. These are solved using a sequential quadratic programming method with the choice of the regularization parameters involved based on the discrepancy principle or the L-curve criterion. It was found that in order to produce a stable and robust numerical solution the first-order regularization smoothness constraint should be employed.

1. INTRODUCTION

The purpose of this work is to demonstrate that a non-destructive evaluation technique based on electrical impedance tomography (EIT) can be effectively applied to image corrosion damage in materials. In this paper, the EIT is used to develop a method to determine material loss occurring on the (inaccessible) portion $\gamma \subset \partial\Omega$ of the boundary $\partial\Omega$ of the material $\Omega \subset R^2$ by measuring voltages and currents (Cauchy data) on the remaining (accessible) portion $\Gamma = \partial\Omega - \gamma$. Therefore, we consider the Laplace equation in a two-dimensional damaged finite plate Ω for the potential u, namely,

$$\nabla^2 u = 0, \quad \text{in } \Omega \tag{1}$$

subject to the boundary conditions

$$u = f, \quad \frac{\partial u}{\partial n} = g, \quad \text{on } \Gamma \tag{2}$$

$$\alpha u + \beta \frac{\partial u}{\partial n} = h, \quad \text{on } \gamma \tag{3}$$

where f, g, h and α, β are prescribed functions such that $\alpha\beta \geq 0$, $\alpha^2 + \beta^2 \neq 0$, and n is the outward normal to the boundary $\partial\Omega$. In eqns (2) and (3), Γ and

γ are, in general, two simple arcs having in common the endpoints only. This problem occurs in several contexts, such as corrosion detection by electrostatic measurements, see Kaup and Santosa (1995).

The uniqueness in determining γ in the problem (1)-(3) when $\alpha = 1$, $\beta = 0$ or $\alpha = 0$, $\beta = 1$, follows from the unique analytical continuation property for the Laplace equation, see Beretta and Vessella (1998). The second theoretical issue is the stability. Unfortunately, our inverse problem is severely ill-posed, see Aparicio and Pidcock (1996), and we cannot expect good stability with the usual topologies because an ill-posed Cauchy problem for the Laplace equation is involved. In fact, Alessandrini (1997) showed that the most one can hope for is logarithmic continuous dependence of γ on the Cauchy data f and g and further, this stability does not improve if one takes many boundary measurements.

Prior to this study, numerical methods were devised for a corroded insulated material, i.e. zero Neumann condition $\alpha = 0$, $\beta = 1$, $h = 0$, see Aparicio and Pidcock (1996). They assumed the potential u to be monotonic along the unknown curve γ and presented two numerical methods for determining an insulated corroded boundary. The first one solves the problem in a closed form and was used to define a parameter that describes the ill-posedness of the problem. The effect of this parameter on a second method based on inverse mapping was thereafter investigated. Both methods reflected the ill-posedness of the problem, but they failed to produce stable solutions even with the additional *a priori* assumption of the unknown $u_{|_\gamma}$ being monotonic. Recently, for a corroded perfect conductor material, i.e. zero Dirichlet condition $\alpha = 1$, $\beta = 0$, $h = 0$, Hon and Wu (2000) approximated the solution $u(x, y)$ as a linear combination of harmonic functions and determined a curve $Y = \{(x, y) \in \overline{\Omega} \mid u(x, y) = 0\}$. However, their solution was found to be highly unstable when noise was introduced in the input data f and g. Further, this method of solution does not seem to be easily extendable when the corroded part is insulated, as in such a situation one will have to determine a curve $Y \subset \overline{\Omega}$ on which $\frac{\partial u}{\partial n} |_Y = 0$ and this becomes complicated. Therefore, the purpose of this paper is to develop a **stable** and robust numerical solution for the ill-posed problem (1)-(3). Either the electric voltage $f(\not\equiv$constant) or current flux $g(\not\equiv 0)$ can be prescribed on Γ in eqn.(2), with the other one being measured as additional information. For the discretisation of the problem (1)-(3) it is particularly advantageous to use the boundary element method (BEM) since we are dealing with a boundary value problem and the discretisation of the boundary only is the essence of the BEM.

2. THE BOUNDARY ELEMENT METHOD

Using Green's formula for eqn.(1) we obtain

$$\eta(p)u(p) = \int_{\partial\Omega} [G(p,p')\frac{\partial u}{\partial n}(p') - u(p')\frac{\partial G}{\partial n_{p'}}(p,p')]dS_{p'}, \quad p \in \overline{\Omega} \tag{4}$$

where $\eta(p)$ is a coefficient function which is equal to 1 if $p \in \Omega$ and 0.5 if $p \in \partial\Omega$

(smooth). In eqn.(4), G is the fundamental solution for the Laplace eqn.(1) which in two-dimensions is given by $G(p,p') = -\frac{1}{2\pi}\ln \mid p-p' \mid$. Using the boundary data (2) we obtain from eqn.(4)

$$\eta(p)u(p) = \int_\Gamma [G(p,p')g(p') - f(p')\frac{\partial G}{\partial n_{p'}}(p,p')]dS_{p'}$$
$$+ \int_\gamma [G(p,p')\frac{\partial u}{\partial n}(p') - u(p')\frac{\partial G}{\partial n_{p'}}(p,p')]dS_{p'}, \quad p \in \overline{\Omega}. \tag{5}$$

We discretise the boundary $\partial\Omega$ in a collection of K boundary elements, namely, $S \approx \cup_{j=1}^{K} S_j$, where $S_j = [p_{j-1}, p_j]$ are straight-line segments. For simplicity, we also adopt a constant BEM approximation in which the unknowns u and $\frac{\partial u}{\partial n}$ are assumed constant over each boundary element S_j and take their values at the midpoints $\tilde{p}_j = (p_j + p_{j-1})/2$, namely,

$$u(p) \equiv u(\tilde{p}_j) = u_j, \quad \text{and} \quad \frac{\partial u}{\partial n}(p) \equiv \frac{\partial u}{\partial n}(\tilde{p}_j) = u'_j, \quad p \in [p_{j-1}, p_j]. \tag{6}$$

Based on the above BEM approximations (6), eqn.(5) becomes

$$\eta(p)u(p) = \sum_{j=1}^{N}[A_j(p)u'_j + B_j(p)u_j] + \sum_{j=N+1}^{M+N}[A_j(p)g_j + B_j(p)f_j], \quad p \in \overline{\Omega} \tag{7}$$

where $f_j = f(\tilde{p}_j)$, $g_j = g(\tilde{g}_j)$,

$$A_j(p) = \int_{S_j} G(p,p')dS_j(p'), \quad B_j(p) = -\int_{S_j} \frac{\partial G}{\partial n_{p'}}(p,p')dS_j(p'), \tag{8}$$

M is the number of boundary elements on Γ, N is the number of boundary elements on γ, and thus $K = M+N$. Collocating eqn.(7) at the boundary nodes $\tilde{p}_i$ for $i = \overline{1,K}$, and eqn.(3) at the boundary nodes $\tilde{p}_j$ for $j = \overline{1,N}$, we obtain

$$\sum_{j=1}^{N}[A_{ij}u'_j + B_{ij}u_j] + \sum_{j=N+1}^{M+N}[A_{ij}g_j + B_{ij}f_j] = 0, \quad i = \overline{1,K} \tag{9}$$

$$\alpha_j u_j + \beta_j u'_j = h_j, \quad j = \overline{1,N} \tag{10}$$

where $\alpha_j = \alpha(\tilde{p}_j)$, $\beta_j = \beta(\tilde{p}_j)$, $h_j = h(\tilde{p}_j)$,

$$A_{ij} = \int_{S_j} G(\tilde{p}_i,p')dS_j(p'), \quad B_{ij} = -\int_{S_j} \frac{\partial G}{\partial n_{p'}}(\tilde{p}_i,p')dS_j(p') - \delta_{ij}\eta_j, \tag{11}$$

$\eta_j = \eta(\tilde{p}_j)$ and δ_{ij} is the Kronecker delta tensor. In eqn.(10), $\alpha_j^2 + \beta_j^2 \neq 0$ and let us assume, for simplicity, that $\beta_j \neq 0$ and, in fact, take $\beta_j = 1$ for $j = \overline{1,N}$. Then introducing (10) into (9) we obtain a system of K equations, namely,

$$\sum_{j=1}^{N}[B_{ij} - \alpha_j A_{ij}]u_j + \sum_{j=1}^{N} A_{ij}h_j + \sum_{j=N+1}^{M+N}[A_{ij}g_j + B_{ij}f_j] = 0, \quad i = \overline{1,K}. \tag{12}$$

For a given initial guess $p_1^{(0)}$,...,$p_{N-1}^{(0)}$, we write the system of eqns (12) as

$$\sum_{j=1}^{N}[B_{ij}-\alpha_j A_{ij}]u_j+\sum_{j=N+1}^{M+N}A_{ij}u'_j=-\sum_{j=1}^{N}A_{ij}h_j-\sum_{j=N+1}^{M+N}B_{ij}f_j,\quad i=\overline{1,K} \tag{13}$$

where we have replaced the measured flux data g_j with the control variable u'_j. Alternatively, we could have worked with the control variable u_j replacing f_j. Expression (13) is a linear system of K equations with K unknowns, namely, u_j for $j=\overline{1,N}$, and u'_j for $j=\overline{(N+1),K}$. Solving this system using for example a Gaussian elimination method we produce in particular the values of $u_j^{'(c)}$ for $j=\overline{(N+1),K}$, where the superscript $^{(c)}$ denotes the calculated value of the flux on the boundary Γ. We can then minimize the Tikhonov functional

$$\text{Objf}(p_1,...,p_{N-1})=\sum_{j=N+1}^{K}(u_j^{'(c)}-g_j^{\epsilon})^2+\lambda\sum_{j=1}^{N}\mid p_j-p_{j-1}\mid^2 \tag{14}$$

where $\lambda\geq 0$ is the regularization parameter and $\underline{g}^{\epsilon}$ represents the noisy measurement data for the exact $\underline{g}$. The minimization of the functional (14) is performed using the NAG routine E04UCF, which is designed to minimize an arbitrary smooth function subject to constraints using a sequential quadratic programming iterative method. When $\lambda=0$, based on the discrepancy principle, see Morozov (1966), we stop the iterative process for the iteration number k for which

$$\text{Objf}(p_1^{(k+1)},...,p_{N-1}^{(k+1)})\leq\epsilon^2\leq\text{Objf}(p_1^{(k)},...,p_{N-1}^{(k)}) \tag{15}$$

where $\epsilon=\mid \underline{g}^{\epsilon}-\underline{g}\mid$. The inclusion of the zeroth-order regularizing term of the form $\mu\sum_{j=1}^{N-1}\mid p_j\mid^2$ in (14) did not significantly improved the results and therefore is not considered herein. When $\lambda>0$, its choice is based on the L-curve criterion, see Hansen (1992).

3. NUMERICAL RESULTS AND DISCUSSION

In this section we consider the case when the unknown boundary γ is the graph of an unknown function $y:[0,l]\rightarrow R$ taking the $x-$axis to pass through the endpoints $y(0)=y(l)=0$ of γ and fixing the origin at $x=0$. Thus the endpoints of the boundary elements S_j on γ will have the known $x-$coordinates $x_j=jl/N$ for $j=\overline{0,N}$. Further, since $y(0)=y(l)=0$, the functional (14) will depend on only $(N-1)$ unknowns, y_1,...,y_{N-1}. We consider that the clean (undamaged) material at the time $t=0$ of installment in an engineering environment is a circle of radius 1, namely, $\Omega_0=\{(x,y)\mid(x-1)^2+y^2<1\}$, which may represent a circular plate, or the cross-section of a long circular cylindrical pipe. At the steady-state, as $t\rightarrow\infty$, the domain becomes corroded and degenerates into the damaged domain Ω. We assume that the upper semicircular part $\Gamma=\{(x,y)\mid(x-1)^2+y^2=1,y\geq 0\}$ remains uncorroded and is known, whilst the corroded

part $\gamma = \partial\Omega - \Gamma$ is unknown, but remains within the initial configuration Ω_0. Thus $l = 2$ and the simple bounds on the unknown variables read as

$$-\frac{2}{N}[j(N-j)]^{1/2} < y_j < \frac{2}{N}[j(N-j)]^{1/2}, \quad j = \overline{1,(N-1)} \tag{16}$$

In order to illustrate a typical benchmark inversion we consider an insulated damaged material, in which the corroded boundary γ is given by the graph of the function $y : [0,2] \to R$,

$$y(x) = \begin{cases} -(x/2 - x^2)^{1/2}, & 0 \le x \le 1/2 \\ (2x - x^2 - 3/4)^{1/2}, & 1/2 \le x \le 3/2 \\ -(7x/2 - x^2 - 3)^{1/2}, & 3/2 \le x \le 2 \end{cases} \tag{17}$$

We consider a non-constant voltage $f = x = \cos(\theta)$, where $\theta \in [0, \pi]$ is the angular polar coordinate, prescribed on Γ which, a direct problem solution, i.e. when γ is known, based on solving the BEM system of eqns (13) using a Gaussian elimination gives rise to the non-zero current $g(\theta)$ on Γ shown in Fig.1. From this figure it can be seen that the mesh size $M = N = 40$ is sufficiently fine for achieving very good accuracy and it was kept fixed in the following inversion. The data g shown with ($\circ\ \circ\ \circ$) in Fig.1, was then perturbed by $p \in \{1, 2, 3\}$ percent Gaussian normally distributed multiplicative random noise as $\underline{g}^{\epsilon} = \underline{g} + \underline{\epsilon}$, generated using the NAG routine G05DDF, with zero mean and standard deviation $\underline{\sigma} = (\sigma_j)_{j=\overline{(N+1),K}}$, where $\sigma_j = p \mid g_j \mid /100$.

The objective least-squares functional (14) has been minimized subject to the constraints (16) using the NAG routine E04UCF.

3.1 The case $\lambda = 0$

The initial guess for $y(x)$ was taken to be the constant -0.15 for $x \in (0, 1/2) \cup (3/2, 2)$, and the constant 0.25 for $x \in [1/2, 3/2]$. These values correspond to close values of the mean between the maximum and minimum $y-$coordinates of γ on the above intervals. When $p = 0$ the final number of iterations, k_f, at which the NAG routine E04UCF finds an optimal numerical solution was obtained to be at $k_f = 702$ with the minimum values of Objf $= 1.4D - 9$. When noise is present in the input data the iterative process should be stopped according to some criterion and in this subsection we have used the discrepancy principle given by eqn.(15). The optimal truncated iteration numbers k_{dp} were found to be 11 and 10 for $p = 1$ and 2, which correspond to values of the noise levels of $\epsilon = 0.0248$ and 0.0497, respectively.

Figure 2 shows the numerically retrieved boundary γ for $p \in \{0, 1, 2\}$ in comparison with its exact target given by eqn.(17). From this figure it can be seen that the numerical solutions appear stable and consistent with the amount of noise p included in the input data g, and that they converge to the exact target given by eqn.(17), as p decreases.

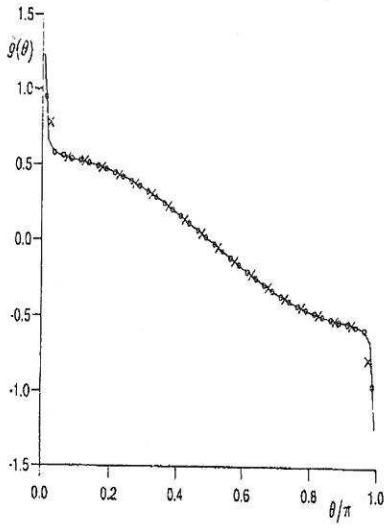

Figure 1: The values of the current flux $g(\theta)$ on Γ obtained for various uniform BEM discretisations, namely, $(\times\ \times\ \times)$ $M = N = 20$, $(\circ\ \circ\ \circ)$ $M = N = 40$, and (---) $M = N = 80$.

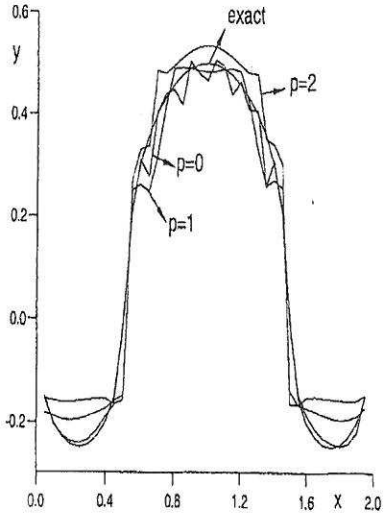

Figure 2: The numerically retrieved boundary γ for $p \in \{0, 1, 2\}$ in comparison with its exact target (17), in the case $\lambda = 0$.

However, this numerical solution was found to be dependent on the initial guess for $y(x)$. Relatively small variations (less than 5%) in the initial guess chosen above did not significantly modify the numerical results, but other initial guesses produced significant unstable solutions, especially when noise was introduced in the input data. Such situations may occur when the routine is trapped in a local minimum and fails (indicated by the `ifail` counter signal) to produce an optimal solution. Therefore, whenever the routine signalled such a failure the numerically obtained results were discarded and a new initial guess was investigated. Alternatively, in order to overcome this lack of robustness, one can employ the first-order regularization method, i.e. $\lambda > 0$, as described in the next subsection.

3.2 The case $\lambda > 0$

The initial guess was taken to be the constant 0.0, and the algorithm was found to be robust, as other initial guesses produced the same numerically convergent results. In the functional (14), the choice of the regularization parameter $\lambda > 0$ is crucial for achieving the stability of the numerical solution, and in this subsection we have used an L-curve type criterion, see Hansen (1992), which plots on a log-log scale the least-squares gap $\mid \underline{u}'^{(c)} - \underline{g}^{\epsilon} \mid$ versus the norm of the derivative of the solution, $\mid \underline{y}' \mid$, for various values of λ. Figure 3 shows the L-curve plots for $p \in \{1, 2, 3\}$. The optimal values of λ are then chosen at the corners of these curves in order to balance the over-smooth regions, i.e. λ too large, and the under-smooth regions, i.e. λ too small. This is confirmed in Fig.4 which shows the accuracy error-norms $\mid \underline{y} - \underline{y}^{(exact)} \mid$, as functions of λ, for $p \in \{1, 2, 3\}$.

Figure 5 shows the numerically retrieved boundary γ obtained using the optimal values λ_{opt} shown in Fig.3 for $p \in \{1, 2, 3\}$, in comparison with its exact target (17). From this figure it can be seen that the numerical solutions are stable and consistent with the amount of noise p included in the input data g, and that they converge to the exact target given by eqn.(17) as p decreases.

We have also investigated the situation when γ is piecewise-smooth as given by the graph of the function $y : [0, 2] \rightarrow R$,

$$y(x) = \begin{cases} 0, & x \in [0, 1/2) \cup (3/2, 2] \\ (2x - x^2 - 3/4)^{1/2}, & x \in [1/2, 3/2] \end{cases} \tag{18}$$

and, as illustrated in Fig.6, the same good stability and accuracy between the numerical solution and the exact target (18) were obtained. In this figure the optimal regularization parameters were chosen according to the L-curve criterion and were found to be $\lambda_{opt} = 5 \times 10^{-3}$ for $p = 1$ and $\lambda_{opt} = 10^{-2}$ for $p \in \{2, 3\}$. The corner points $(0.5, 0)$ and $(1.5, 0)$ are, as expected, rounded-off since the minimization of the first-order regularization functional (14) imposes the numerical solution to be smooth.

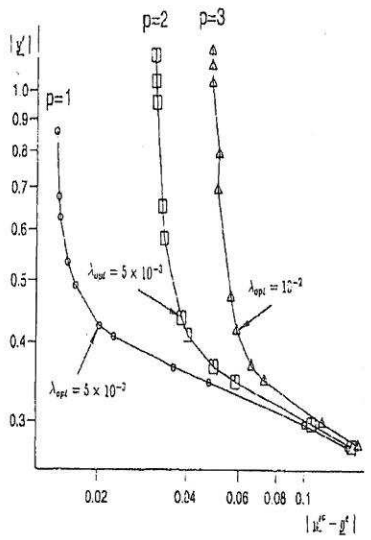

Figure 3: The L-curve plots of $\mid \underline{u'^{\epsilon}} - \underline{g^{\epsilon}} \mid$ versus the norm of the first-order derivative, $\mid \underline{y'} \mid$, for various values of $\lambda \in \{10^{-k}; k = \overline{0,5}\} \cup \{5 \times 10^{-k}; k = \overline{1,5}\}$ for $p \in \{1, 2, 3\}$.

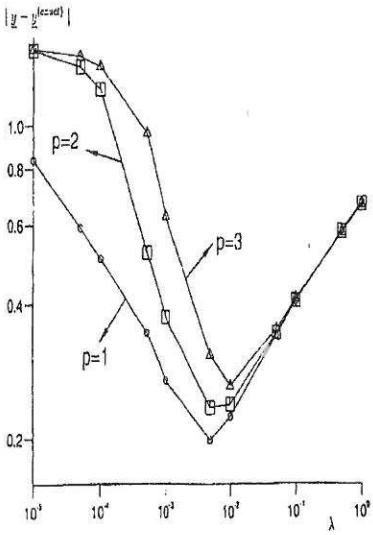

Figure 4: The accuracy error-norms $\mid \underline{y} - \underline{y}^{(exact)} \mid$, as functions of λ, for $p \in \{1, 2, 3\}$.

4. CONCLUSIONS

In this paper the inverse boundary determination in potential corroded materials which requires the determination of the location, size and shape of an unknown, or partially unknown, portion $\gamma \subset \partial\Omega$ of the boundary $\partial\Omega$ of a solution domain $\Omega \subset R^2$ in which Laplace's equation holds from additional Cauchy data on the remaining portion of the boundary $\Gamma = \partial\Omega - \gamma$, has been investigated numerically. This inverse problem was discretised using the boundary element method (BEM). Since the resulting system of equations is ill-conditioned, constrained minimization problems based on least-squares, zeroth- or first-order regularization have been formulated. These problems have been solved using a sequential quadratic programming method with the choice of the regularization parameters involved based on the discrepancy principle or the L-curve criterion. It was found that in order to produce a stable and robust numerical solution the first-order regularization smoothness constraint needed to be employed. Further work will be concerned with extending the numerical method of this study to the retrieval of more complex boundaries which are not graphs of functions and also to include transient effects.

Acknowledgement

The first author would like to acknowledge the Department of Mathematical and Computer Sciences at Colorado School of Mines and some financial support from the Leverhulme Trust for this research which was performed whilst on study leave from the University of Leeds.

REFERENCES

Alessandrini, G. (1997) Examples of instability in inverse boundary-value problems, *Inverse Problems* **13**, 887-897.

Aparicio, N.D. and Pidcock, M. (1996) The boundary inverse problem for the Laplace equation in two dimensions, *Inverse Problems* **12**, 565-577.

Beretta, E. and Vessella, S. (1998) Stable determination of boundaries from Cauchy data, *SIAM J.Math.Anal.* **30**, 220-232.

Hansen, P.C. (1992) Analysis of discrete ill-posed problems by means of the L-curve, *SIAM Rev.* **34**, 561-580.

Hon, Y.C. and Wu, Z. (2000) A numerical computation for inverse boundary determination problem, *Eng.Anal.Boundary Elements* **24**, 599-606.

Kaup, P. and Santosa, F. (1995) Nondestructive evaluation of corrosion damage using electrostatic boundary measurements, *J.Nondestruct.Eval.* **14**, 127-136.

Morozov, V.A. (1966) On the solution of functional equations by the method of regularization, *Soviet Math.Dokl.* **7**, 414-417.